2006

# Heparin Modulates the 99-Loop of Factor IXa: EFFECTS ON REACTIVITY WITH ISOLATED KUNITZ-TYPE INHIBITOR DOMAINS

Pierre F. Neuenschwander
*University of Texas Health Center at Tyler*

Stephen R. Williamson
*University of Texas Health Center at Tyler*

Armen Nalian
*Stephen F Austin State University*

Kimberly J. Baker-Deadmond
*University of Texas Health Center at Tyler*

Follow this and additional works at: https://scholarworks.sfasu.edu/biology

Part of the Biochemistry Commons, Enzymes and Coenzymes Commons, and the Molecular Biology Commons

Tell us how this article helped you.

## Repository Citation

# Heparin Modulates the 99-Loop of Factor IXa
## EFFECTS ON REACTIVITY WITH ISOLATED KUNITZ-TYPE INHIBITOR DOMAINS*[S]

**Pierre F. Neuenschwander**[‡1], **Stephen R. Williamson**[‡], **Armen Nalian**[§], and **Kimberly J. Baker-Deadmond**[‡]

*From the* ‡*Department of Biochemistry, Biomedical Research Program, The University of Texas Health Science Center, Tyler, Texas 75708 and the* §*Department of Biotechnology, Stephen F. Austin State University, Nacogdoches, Texas 75962*

Reactivity of factor IXa with basic pancreatic trypsin inhibitor is enhanced by low molecular weight heparin (enoxaparin). Previous studies by us have suggested that this effect involves allosteric modulation of factor IXa. We examined the reactivity of factor IXa with several isolated Kunitz-type inhibitor domains: basic pancreatic trypsin inhibitor, the Kunitz inhibitor domain of protease Nexin-2, and the first two inhibitor domains of tissue factor pathway inhibitor. We find that enhancement of factor IXa reactivity by enoxaparin is greatest for basic pancreatic trypsin inhibitor (>10-fold), followed by the second tissue factor pathway inhibitor domain (1.7-fold) and the Kunitz inhibitor domain of protease Nexin-2 (1.4-fold). Modeling studies of factor IXa with basic pancreatic trypsin inhibitor suggest that binding of this inhibitor is sterically hindered by the 99-loop of factor IXa, specifically residue Lys[98]. Slow-binding kinetic studies support the formation of a weak initial enzyme-inhibitor complex between factor IXa and basic pancreatic trypsin inhibitor that is facilitated by enoxaparin binding. Mutation of Lys[98] to Ala in factor IXa results in enhanced reactivity with all inhibitors examined, whereas almost completely abrogating the enhancing effects of enoxaparin. The results implicate Lys[98] and the 99-loop of factor IXa in defining enzyme inhibitor specificity. More importantly, these results demonstrate the ability of factor IXa to be allosterically modulated by occupation of the heparin-binding exosite.

Factor IXa (fIXa)[2] is a vitamin K-dependent blood coagulation factor that is essential for the amplification or "consolidation" phase of blood coagulation (1, 2). As with other blood coagulation factors (namely factors VIIa, Xa, and thrombin) fIXa is a member of the serine protease family and shares a high degree of homology with trypsin. Despite this homology, the blood coagulation enzymes differ drastically from trypsin in that their activities are profoundly modulated by the binding of various protein and non-protein cofactors. In the case of fIXa, the ability of activated factor VIII (fVIIIa), anionic phospholipid, and ionic calcium to enhance the procoagulant activity of fIXa is well documented (3–6); resulting in a $10^9$-fold increase in activity of fIXa. The molecular details of this conversion have not been defined in total and are the subject of intense investigation by numerous groups.

The major inhibitor of fIXa in plasma is antithrombin, whose reactivity with fIXa essentially requires heparin (7–9). Heparin is known to bind to antithrombin and sterically alter its conformation to allow this serpin to react with its target (10–13). Heparin also binds to fIXa (14) allowing long chains of heparin to additionally catalyze the interaction of fIXa with antithrombin via the formation of bridged complexes where heparin acts as a "template." Recently, we have shown that low molecular weight heparin binding to fIXa enhances reactivity of fIXa with the Kunitz-type inhibitor BPTI (15), suggesting that oligosaccharide binding can also allosterically modulate the fIXa active site region. In this study we examine in greater detail the ability of heparin to modulate fIXa reactivity toward several isolated Kunitz-type inhibitor domains. We show that the modulatory effect of heparin can be completely abrogated by mutating a single amino acid residue in the 99-loop region of the extended fIXa active site cleft outside of the heparin binding exosite.

## EXPERIMENTAL PROCEDURES

*Materials*—Factor IXaβ, factor VIIa, factor XIa, and the factor X activator from Russell's Viper venom were purchased from Hematologic Technologies Inc. (Essex Junction, VT). Recombinant soluble tissue factor (the extracellular domain of tissue factor) was expressed and purified from bacteria as previously described (16). Factor Xa was prepared from plasma-derived factor X as previously described (17). Enoxaparin (Lovenox®) was purchased from Aventis Pharmaceuticals (Bridgewater, NJ). Purified heparin-derived oligosaccharides of 6, 10, 14, and 18 saccharide units (H6, H10, H14, and H18) were prepared and characterized essentially as described (18–20) and were a generous gift of Dr. Steven T. Olson, University of Illinois, Chicago, IL. Bovine serum albumin (Fraction V, fatty acid free) was from Calbiochem (La Jolla, CA), and ethylene glycol was from Fisher Scientific. The chromogenic substrate CBS 31.39 ($CH_3SO_2$-D-LGR-$p$NA) was purchased from Diagnostica Stago (Parsippany, NJ). All other reagents were of the highest quality available.

[S] The on-line version of this article (available at http://www.jbc.org) contains supplemental Table S1 and Figs. S1–S3.

[1] To whom correspondence should be addressed: Biomedical Research Lab C8, The University of Texas Health Science Center at Tyler, 11937 US Hwy. 271, Tyler, TX 75708. Tel.: 903-877-7678; Fax: 903-877-7679; E-mail: Pierre.Neuenschwander@uthct.edu.

[2] The abbreviations used are: FIXa, factor IXa; BPTI, basic pancreatic trypsin inhibitor; PN2-KPI, the isolated Kunitz-type inhibitor domain from protease nexin-2; TFPI, tissue factor pathway inhibitor; TFPI-K1, the isolated first Kunitz-type inhibitor domain of TFPI; TFPI-K2, the isolated second Kunitz-type inhibitor domain of TFPI; WT, wild-type; MES, 4-morpholineethanesulfonic acid; MOPS, 4-morpholinepropanesulfonic acid; Tricine, N-[2-hydroxy-1,1-bis(hydroxymethyl)ethyl]glycine.

*Construction and Expression of Recombinant Inhibitors*—
Appropriate expression clones encoded for: BPTI (59 amino acids) (21, 22), PN2-KPI (61 amino acids corresponding to residues 285–344 of Protease Nexin-2) (23), TFPI-K1 (58 amino acids corresponding to residues 50–107 of TFPI) (24), and TFPI-K2 (59 amino acids corresponding to residues 121–178 of TFPI) (24). Each construct was directionally cloned into pET11a (Novagen) and verified by sequencing. Inhibitors were expressed as inclusion bodies in *Escherichia coli* strain BL21(DE3). Transformed bacterial cells were first grown to log phase at 37 °C in TB media containing 50 $\mu$g/ml carbenicillin. Protein expression was induced by addition of isopropyl 1-thio-$\beta$-D-galactopyranoside to 0.5 mM (0.1 mM for TFPI-K1) and the cells were allowed to continue growing for 4 h at 37 °C.

Inclusion bodies were isolated essentially as described (25) and solubilized with 6 M guanidine HCl containing 20 mM dithiothreitol, 50 mM Tris-HCl, pH 8.0, and 1 mM EDTA to obtain a total protein concentration of roughly 20 mg/ml. The solution was then clarified by centrifugation (16,000 × *g* for 30 min) and oxidative refolding (26) of each protein preparation was performed by rapid dilution into 20 volumes of buffer containing 50 mM Tris-HCl, pH 8.0, 1 M guanidine HCl, 1 mM EDTA, 2.5 mM oxidized glutathione (Sigma), and 1 mM dithiothreitol. The diluted protein solution was incubated at room temperature for 6 h with slow stirring for completion of protein refolding followed by exhaustive dialysis into an appropriate buffer for ion-exchange chromatography.

*Construction and Expression of Wild-type and Mutant fIX*—
The coding sequence for wild-type fIX in pBR322 (27) was a generous gift of Dr. Earl Davie (University of Washington). The fIX coding sequence was removed into the mammalian expression vector pcDNA3 (Invitrogen) and sequenced to verify the correct orientation. This construct (pFN04) was used for expression of wild-type fIX as well as PCR-based mutagenesis (28) to generate fIXK98A essentially as previously described for constructing fVII mutants (29). Expression constructs were transfected into human 293 cells using Lipofectin® (Invitrogen) and high expressing clones isolated by limiting dilution.

*Protein Purifications*—Purification of refolded BPTI was accomplished by ion-exchange chromatography using Mono-S HR 5/5 (Amersham Biosciences) in 20 mM Tris-HCl, pH 8.0. The column was developed with a 0–1 M NaCl gradient and BPTI eluted as a single peak at roughly 0.43 M NaCl. The specific activity of recombinant BPTI preparations was equivalent to or better than that of commercial preparations of aprotinin (not shown). Purification of refolded PN2-KPI and TFPI-K2 was accomplished by ion-exchange chromatography using Mono-Q HR 5/5 (Amersham Biosciences) in 20 mM MES, pH 6.0. In both cases the column was developed with a 0–0.5 M NaCl gradient. PN2-KPI eluted at roughly 90 mM NaCl and TFPI-K2 eluted at roughly 50 mM NaCl. Purification of refolded TFPI-K1 was accomplished by affinity chromatography over a trypsin-agarose column. Trypsin-agarose was prepared by coupling 20 mg of L-1-tosylamido-2-phenylethyl chloromethyl ketone-treated trypsin (Worthington Biochemicals) to 2.5 ml of Affi-Gel 10 in 100 mM MOPS, pH 7.4, 10 mM CaCl$_2$, and 100 $\mu$g/ml leupeptin overnight at 4 °C. This was followed by blocking non-reacted sites with 1 M ethanolamine-HCl, pH 8.0.

Refolded TFPI-K1 was loaded onto the prepared trypsin-agarose column in 50 mM Tris-HCl, pH 7.5, 100 mM NaCl. The column was extensively washed with the same buffer before eluting the inhibitor with 10 mM HCl, pH 2.1, 100 mM NaCl. The pH of the eluted fractions was immediately neutralized with 0.02 volumes of 2 M Tris buffer. All inhibitors were judged >95% pure by SDS-PAGE.

Recombinant human wild-type fIX and fIXK98A were isolated from 293 cell supernatants using a combination of ion-exchange and heparin affinity chromatography. A 10-fold concentrate of cell supernatant was diluted 2-fold with deionized water to reduce the ionic strength before loading a 150-ml DEAE FF Sepharose (Amersham Biosciences) column equilibrated in 25 mM sodium citrate, pH 6.0, 33 mM NaCl, and 1 mM benzamidine. After loading, the column was extensively washed in the same buffer before elution of the fIX protein with a 0.033–0.4 M NaCl gradient over 10 column volumes. The fIX protein peak was identified by clotting activity, pooled, and dialyzed *versus* 50 mM Tris-HCl, pH 7.5, 100 mM NaCl before heparin affinity chromatography using either POROS® HE2 (Applied Biosystems) or HiPrep™ Heparin FF 16/10 (Amersham Biosciences) and eluting with a NaCl gradient. Wild-type fIX and fIXK98A both eluted as single peaks at roughly 0.46 M NaCl.

Wild-type and mutant fIX proteins were activated with the purified factor X activator from the venom of Russell's viper, which also cleaves fIX after Arg[180] to generate active enzyme (fIXa$\alpha$). The activated enzyme was purified away from the venom protease by subsequent heparin affinity chromatography essentially as described above using HiTrap™ Heparin HP (Amersham Biosciences). Although the activation peptide remains attached to the light chain of fIXa$\alpha$, this enzyme retains 100% amidolytic activity compared with fIXa$\beta$ (activation peptide proteolytically removed) and is comparable with fIXa$\beta$ in kinetics of inhibition by Kunitz-type inhibitors (see "Results"). Unless indicated otherwise, the fIXa$\alpha$ form was used in experiments.

*Clotting Assays*—Coagulant activities of wild-type and mutant fIXa proteins were assayed by a standard single-stage clotting assay using a Coag-a-mate XM (Organon Teknika) coagulometer, fIX-deficient plasma (George King Biomedical), and APTT Reagent (Sigma).

*Reactive Site Titration of Inhibitors*—The active concentration of inhibitor preparations was determined by reactive site titration essentially as described (23) using 10 nM active site-titrated trypsin (30) and S-2222 substrate (Chromogenix, Milano, Italy) to measure residual trypsin activity after a 15-min incubation period. This method assumes a 1:1 stoichiometry of inhibitor and trypsin. Amino acid analysis performed on an initial PN2-KPI preparation indicated an equivalent concentration as that determined by reactive site titration (not shown).

*Active Site Titration of fIXa Enzymes*—Active concentrations of wild-type and mutant fIXa preparations were determined by active site titration using biotin-EGR-ck (Hematologic Technologies Inc.) essentially as described (31). Briefly, wild-type or mutant fIXa (roughly 5 $\mu$M) were incubated with 150 $\mu$M biotin-EGR-ck in 50 mM Tricine, pH 8.0, 200 mM NaCl, 10 mM CaCl$_2$,

$$E + S \underset{k_2}{\overset{k_1}{\rightleftarrows}} ES \overset{k_7}{\longrightarrow} E + P$$
$$+$$
$$I$$

$$k_4 \big\updownarrow k_3 \quad K_i$$

$$EI \underset{k_6}{\overset{k_5}{\rightleftarrows}} EI^*$$

$K_i^*$

$$E + S \underset{k_2}{\overset{k_1}{\rightleftarrows}} ES \overset{k_7}{\longrightarrow} E + P$$
$$+$$
$$I$$

$$k_{10} \big\updownarrow k_9 \quad K_i^*$$

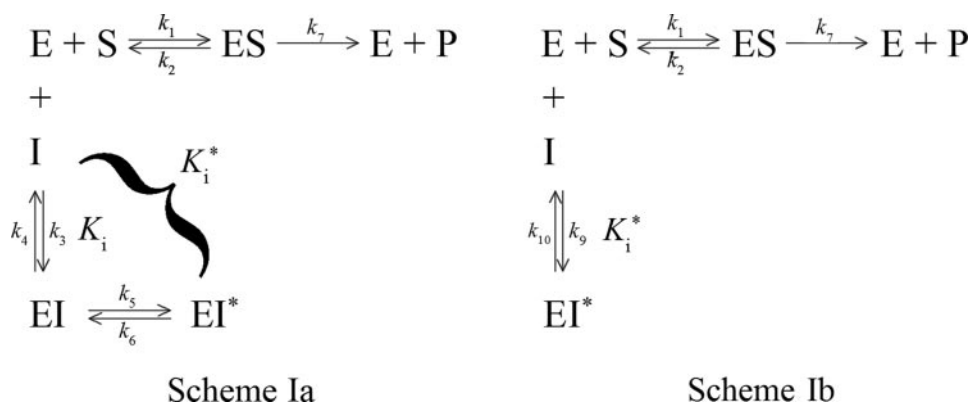$$EI^*$$

Scheme Ia                              Scheme Ib

FIGURE 1. **Reversible slow-binding enzyme inhibition schemes.** Schemes Ia and Ib both describe the reversible slow-binding inhibition of an enzyme ($E$) by an inhibitor (I) resulting in competitive inhibition of substrate (S) binding and the subsequent reduction in product (P) formation (33, 34). Both schemes show the formation of the Michaelis complex ($ES$) as described classically by $k_1$, $k_2$, and $k_7$. In Scheme Ia inhibition of enzyme occurs in two distinct steps: 1) formation of a loose $EI$ inhibitory complex described by $k_3$ and $k_4$, where $k_4/k_3 = K_i$. 2) Isomerization of $EI$ to $EI^*$ described by $k_5$ and $k_6$. In Scheme Ib the binding of inhibitor and isomerization of the complex are simultaneous and not distinguishable. In this case $k_9$ and $k_{10}$ represent the overall on- and off-rate constants. This situation can arise when $k_4$ and $k_3$ are very slow (rate-limiting) compared with $k_5$ and $k_6$. In both schemes the overall inhibition is described by $K_i^*$, which is the final inhibition constant observed at equilibrium of the system.

and 30% ethylene glycol for 24 h at room temperature. Biotin-EGR-fIXa was then quantified by enzyme-linked immunosorbent assay using a goat anti-fIX polyclonal capture antibody and alkaline phosphatase-conjugated streptavidin. These were compared with a standard line made using native fIXa$\beta$ to determine active concentrations for all fIXa enzyme preparations.

*Equilibrium Enzyme Inhibition Assays*—Reversible competitive inhibition of fIXa amidolytic activity at equilibrium was measured at 25 °C using final concentrations of 25 nM fIXa, 5 mM CaCl$_2$ and the indicated concentrations of enoxaparin and inhibitor in the presence of 30% ethylene glycol as previously described (15). The addition of ethylene glycol enhances the enzymatic activity of fIXa toward CBS 31.39 roughly 20-fold (32). Previous studies by us as well as control experiments performed with each inhibitor examined showed that the inclusion of ethylene glycol in the assay has no effect on the reactivity of fIXa with these inhibitors (15). Values of the final equilibrium inhibition constant ($K_{i,eq}$) were estimated as described (15, 29) using Equation 1. This equation describes simple reversible competitive inhibition where $v_o$ is the steady state rate obtained in the absence of inhibitor, $v_s$ is the steady state rate at each concentration of inhibitor, S is the experimental substrate concentration, and $K_m$ is the Michaelis constant for substrate hydrolysis.

$$v_s = v_o \frac{K_{i,eq}(1 + S/K_m)}{I + K_{i,eq}(1 + S/K_m)} \qquad \text{(Eq. 1)}$$

*Slow-binding Enzyme Inhibition Analysis*—Kinetic parameters for slow-binding inhibition were obtained using Equations 2–5 as derived by others (33, 34) and are described in Schemes Ia and Ib (Fig. 1). In both of these schemes the non-covalent enzyme-inhibitor complex, $EI$, isomerizes into $EI^*$; either after significant formation of the $EI$ complex (Scheme Ia) or without significant accumulation of the $EI$ complex (Scheme Ib). In both cases, the overall inhibition constant describing genera-

tion of $EI^*$ is defined as $K_i^*$, which is equivalent to $K_{i,eq}$ obtained from equilibrium experiments (above). In cases following Scheme Ia, the parameter $K_i^*$ can be further broken down to obtain $K_i$, which describes the establishment of the initial "loose" $EI$ complex, $k_5$ and $k_6$ (see below).

Final reaction conditions were the same as described above for equilibrium studies. In these assays, however, the fIXa was preincubated with or without enoxaparin for 15 min at 25 °C in the reaction mixture before the combined addition of inhibitor and substrate at time 0. The absorbance at 405 nm was then monitored for up to 30 min in a ThermoMax microplate reader (Molecular Devices) set at 25 °C to monitor substrate hydrolysis using KINEMAX software (written and kindly provided by Dr. Jolyon Jesty, SUSB, Stony Brook, NY). Data for each generated curve were fitted with the following integrated rate equation describing slow-binding inhibition,

$$A = v_s t + (v_o - v_s)(1 - e^{-k_{obs}t})/k_{obs} + A_o \qquad \text{(Eq. 2)}$$

where $A$ is the absorbance at 405 nm at any time, $t$. Fits of progress curves with Equation 2 yield values for $A_o$ (the initial absorbance at $t = 0$), $v_o$ (the initial rate of substrate hydrolysis), $v_s$ (the steady-state rate of substrate hydrolysis), and $k_{obs}$ (the apparent first-order rate constant for inhibition).

For analyses using Scheme Ia, values of $k_6$ (the reverse rate constant for $EI^*$ isomerization) were determined from progress curves above using the following relationship.

$$k_6 \text{ or } k_{10} = k_{obs}v_s/v_o \qquad \text{(Eq. 3)}$$

Values of $k_5$ and initial $K_i$ (defined as $k_4/k_3$) were then obtained from secondary plots of $k_{obs}$ *versus* I using the following hyperbolic equation.

$$k_{obs} = k_6 + k_5 I/(1 + K_i(1 + S/K_m)) \qquad \text{(Eq. 4)}$$

For analyses using Scheme Ib, values of $k_{10}$ were obtained from progress curves also using Equation 3. However, in these cases $v_o$ does not vary with inhibitor concentration and a plot of $k_{obs}$ *versus* I yields a straight line, indicating conditions where $K_i$ $(1+ S/K_m)$ $\gg$ I. Thus for Scheme Ib $EI$ formation is insignificant and $EI^*$ can be considered formed directly from $E +$ I. For these cases the following linear equation is applicable for obtaining an estimate of $k_9$, the apparent second-order on-rate constant,

$$k_{obs} = k_{10} + k_9 I/(1 + S/K_m) \qquad \text{(Eq. 5)}$$

where the $y$ intercept reflects $k_{10}$ and the slope of the line is equal to $k_9/(1 + S/K_m)$. Alternatively, $k_9$ can be obtained from $K_i^*$, which is equivalent to $K_{i,eq}$ in Equation 1, using the relationship $k_9 = k_{10}/K_i^*$.
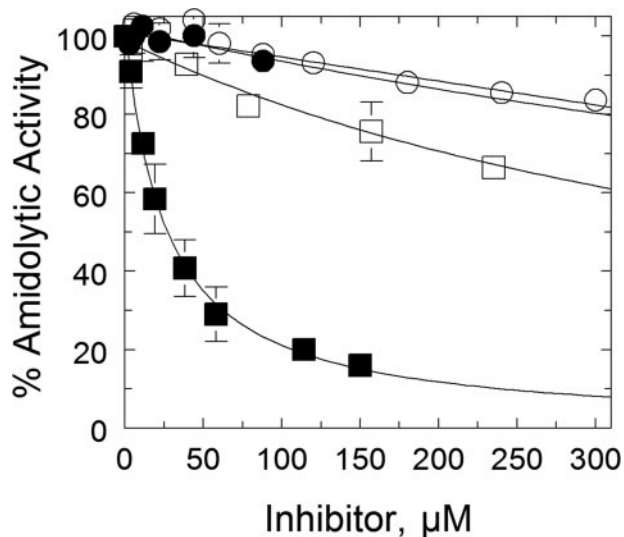
FIGURE 2. **Inhibition of fIXaβ by isolated Kunitz-type inhibitor domains.** FIXaβ (25 nM) was titrated with the indicated concentrations of BPTI (○), TFPI-K1 (●), TFPI-K2 (□), and PN2-KPI (■). The remaining fIXa amidolytic activity at equilibrium was then measured and values were normalized to the activity of fIXa in the absence of inhibitor (100%). Data were fitted with Equation 1 (*lines*) to obtain values of $K_{i,eq}$ (see text).
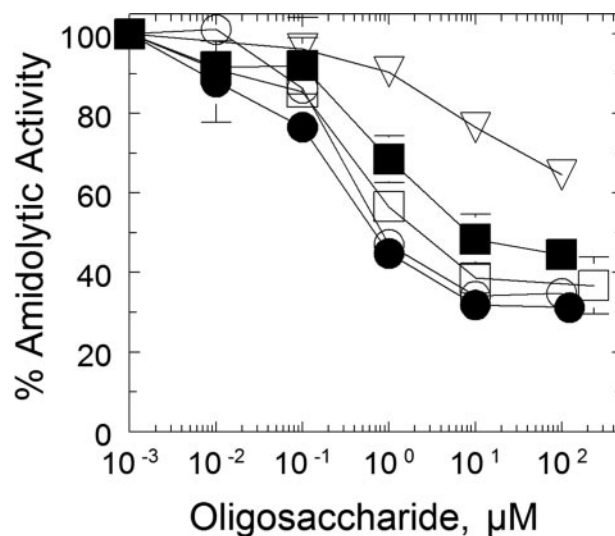


FIGURE 3. **Support of BPTI inhibition of fIXa by short chain oligosaccharides.** The ability of heparin oligosaccharides with progressively shorter chain lengths to support enhancement of fIXa reactivity with BPTI was examined using 25 nM fIXaβ, 308 μM BPTI, and the indicated concentrations of heparin-derived oligosaccharides (18–20) from 0.01 to 200 μM. Saccharide chain lengths were H18 (●), H14 (□), H10 (■), and H6 (▽). Enoxaparin (H15) is shown for comparison (○). The fIXa activities were normalized to the activity of fIXa in the absence of added oligosaccharide.

Although fits with Equations 4 or 5 yield estimates of $k_6$ or $k_{10}$, respectively, the values reported herein were obtained from Equation 3 using the more accurate fits of progress curves to Equation 2 and then verified in fits with Equations 4 or 5. Experimental values of S as well as experimentally determined values of $K_m$ (defined in the traditional manner as $(k_2 + k_7)/k_1$ in Schemes Ia and Ib) were used as necessary in all fitting procedures. All regression procedures were performed using SlideWritePlus 6.0 (Advanced Graphics Software), which uses the Levenberg-Marquardt algorithm.

## RESULTS

Previous studies (15) by us have shown that whereas fIXa is resistant to inhibition by the Kunitz-type inhibitor BPTI, this resistance is somewhat alleviated by enoxaparin, leading to a roughly 10-fold enhancement in the equilibrium inhibition constant. To gain further insight into mechanisms of fIXa selectivity and its modulation by heparin we undertook an examination of the reactivity of fIXa with several isolated Kunitz-type inhibitor domains: BPTI, PN2-KPI, TFPI-K1, and TFPI-K2. Each of these inhibitors was expressed in *E. coli* using standard recombinant techniques, purified to homogeneity and quantified by reactive site titration as described under "Experimental Procedures." The isolated PN2-KPI inhibitor domain was found to react with high affinity toward factor XIa, yielding a $K_{i,eq}$ of roughly 400 pM (see supplemental data). Similarly, preliminary studies indicated that preparations of isolated TFPI-K1 domain inhibited the complex of factor VIIa and soluble tissue factor with high affinity ($K_{i,eq} = 400$ nM) and weakly inhibited factor Xa ($K_{i,eq} > 1.5$ μM). Conversely, the isolated TFPI-K2 domain inhibited factor Xa with high affinity ($K_{i,eq} = 24$ nM) and the factor VIIa-tissue factor complex with reduced affinity ($K_{i,eq} = 7$ μM). These results are consistent with the expected reactivity of the isolated inhibitor domains (35, 36)

and demonstrate the correct folding and inhibitor activity of the inhibitors examined.

The abilities of these isolated Kunitz inhibitor domains to inhibit fIXaβ are compared in Fig. 2. As expected, fIXa exhibited remarkable specificity toward these inhibitors despite their high homology. Of the inhibitors examined, PN2-KPI showed the highest level of reactivity ($K_{i,eq} = 10$ μM), followed by TFPI-K2 ($K_{i,eq} = 336$ μM), BPTI ($K_{i,eq} > 500$ μM), and TFPI-K1 ($K_{i,eq} > 1$ mM). Consistent with our previous observations, enoxaparin was able to enhance the reactivity of fIXa with BPTI more than 10-fold ($K_{i,eq} = 46$ μM). Surprisingly, however, this same level of enhancement by enoxaparin was not observed with any of the other inhibitors examined; TFPI-K2 and PN2-KPI each showed only a small, but consistent, enhancement in reactivity with enoxaparin (1.7- and 1.4-fold, respectively; $K_{i,eq}$ values of 203 and 7 μM) and TFPI-K1 showed no measurable enhancement in reactivity with enoxaparin.

The highly basic nature of BPTI compared with the other isolated Kunitz domains along with its ability to bind to heparin (albeit weakly; $K_d = 172$ μM (15)) raised the potential that enoxaparin, although short (15 saccharide units; H15), may retain some capacity to facilitate the interaction of BPTI with fIXa via a bridging-type mechanism. Although unlikely based on previous equilibrium kinetic studies and the level of enoxaparin used in these experiments (10 μM; or $0.06 \times K_d$ for BPTI binding *versus* $78 \times K_d$ for fIXa binding), this issue was examined by using increasing concentrations of enoxaparin as well as progressively smaller heparin oligosaccharides; H18, H14, H10, and H6 (18–20). As shown in Fig. 3, the typical bell-shaped profile for bridging-type mechanisms was not observed at enoxaparin concentrations ranging from 1 nM to >100 μM. In addition, and of greater significance, is the observation that progressively smaller oligosaccharides do not lose the ability to enhance reactivity of fIXa. These results along with previous
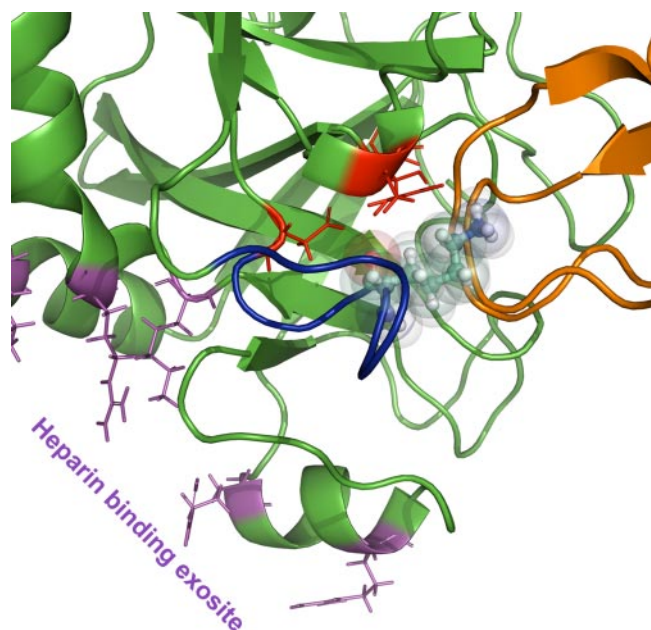
FIGURE 4. **Hypothetical model of the inhibited fIXa-BPTI complex.** A hypothetical fIXa-BPTI complex model was constructed using Discovery Studio software (Accelrys) based on known crystal structures of fIXa (PDB code 1RFN) and fVIIa-BPTI$_{5L15}$ (PDB code 1FAK) using molecular replacement. The structure revealed potential steric hindrance between BPTI and the 99-loop of fIXa, specifically Lys[98] (central ball and stick structure with van der Waals radii). BPTI is depicted in *orange*; fIXa is depicted in *green* with the 99-loop in *blue*; the heparin binding exosite residues in fIXa (14) are depicted as *violet sticks*; and the fIXa active site triad residues (Ser[195], His[57], and Asp[102]) are depicted as *red sticks*.

kinetic studies support the ability of heparin to modulate fIXa reactivity via a mechanism other than bridging, and are consistent with allosteric modulation of the fIXa protease domain.

To gain further insight into the potential mechanism of heparin modulation of fIXa, we prepared a rudimentary hypothetical model of the fIXa-BPTI complex using available crystal structures of BPTI (37), fIXa (38), and the fVIIa-BPTI$_{5L15}$ complex (39). Using the latter structure as a template, superimposition of the native BPTI structure over the mutant BPTI structure along with superimposition of the fIXa structure over the fVIIa structure (Discovery Studio v 1.1; Accelrys Inc.) suggested a constriction of the fIXa active site in a manner that may be expected not to readily accommodate BPTI. The main site of steric hindrance seemed to be with the 99-loop of fIXa, specifically residue Lys[98] (Fig. 4). We hypothesized that heparin binding may act to allosterically modulate the 99-loop of fIXa.

Based on this hypothesis, we examined a mutant of fIXa in which Lys[98] was mutated to Ala (fIXK98A). Wild-type and mutant forms of fIXa were expressed in human 293 cells and purified to >95% homogeneity as judged by SDS-PAGE (Fig. 5A). The fIXK98A mutant was found to retain 100% clotting activity compared with wild-type fIXa (Fig. 5B) and upon activation retained near normal amidolytic activity toward CBS 31.39 substrate (Table 1).

We first examined the kinetics of inhibition of WT fIXa by BPTI using the slow-binding inhibition model (33, 34). In this model (Fig. 1, Scheme Ia) BPTI forms an initial loose inhibitory complex with fIXa (defined by $K_i$ and the rate constants $k_3$ and $k_4$) followed by the slow isomerization of the $E$I complex to $E$I* (defined by the rate constants $k_5$ and $k_6$). This results in overall inhibition of the enzyme as defined by $K_i^*$, which is equivalent to the $K_{i,eq}$ value determined in equilibrium experiments. The progress curves obtained for BPTI inhibition of WT fIXa in the absence and presence of a saturating level of enoxaparin are shown in Fig. 6, *A* and *B*, respectively. The shapes of the progress curves support the slow binding nature of BPTI with recombinant WT fIXa. These curves were identical to control reactions performed with fIXaβ (not shown) and are well described by Equation 2. Values of $k_6$ subsequently obtained using Equation 3 showed no significant differences in the absence or presence of enoxaparin; $k_6 = 2.7 (\pm 1.5) \times 10^{-3}$ s$^{-1}$ without enoxaparin and $1.2 (\pm 0.2) \times 10^{-3}$ s$^{-1}$ with enoxaparin.

As an independent verification of $k_6$ an experiment was performed where 5 μM fIXa was incubated with 231 μM BPTI in the presence of enoxaparin for 20 min, followed by a rapid 1,000-fold dilution into the same buffer also containing enoxaparin. Timed aliquots of this diluted mixture were removed into 1 mM CBS 31.39 substrate to monitor the recovery of enzyme activity over time (Fig. 6B, *inset*). Under these conditions, the BPTI concentration is over 200-fold lower than the apparent $K_{i,eq}$ and thus $k_6$ can be approximated by the rate constant describing recovery of activity (33, 34). Fitting the data with a single exponential equation yielded a value for this rate constant that reasonably supports the value of $k_6$ obtained above ($1.9 \times 10^{-3}$ s$^{-1}$).

From fits of the progress curves in Fig. 6, *A* and *B*, with Equation 2, secondary plots of $k_{obs}$ *versus* BPTI for WT fIXa show little or no curvature (Fig. 6C). This suggests a very high initial $K_i$ value and an indeterminate value for $k_5$. These observations as well as the lack of change in $v_o$ with increasing inhibitor
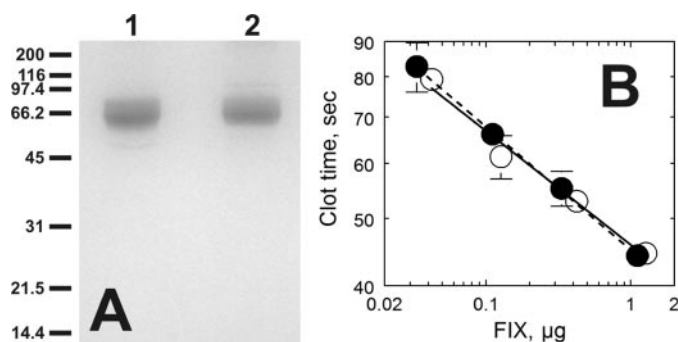


FIGURE 5. *A*, SDS-PAGE analysis of recombinant WT fIX and fIXK98A. Five μg of purified WT fIX (*lane 1*) and fIXK98A (*lane 2*) were loaded onto a 12% polyacrylamide gel under reducing conditions for SDS-PAGE. The resulting gel was stained with Coomassie Brilliant Blue G-250. Molecular weight markers are indicated on the *left*. *B*, clotting activity of fIXK98A *versus* WT fIX. Standard single-stage clotting assays were performed on recombinant WT fIX (○) and fIXK98A (●), which showed equivalent coagulant activity.

**TABLE 1**

**Kinetic parameters for CBS 31.39 hydrolysis by WT fIXa *versus* fIXaK98A**

Obtained by fitting the data with the Michaelis-Menton equation. Values shown are ± S.E., $n = 6$.

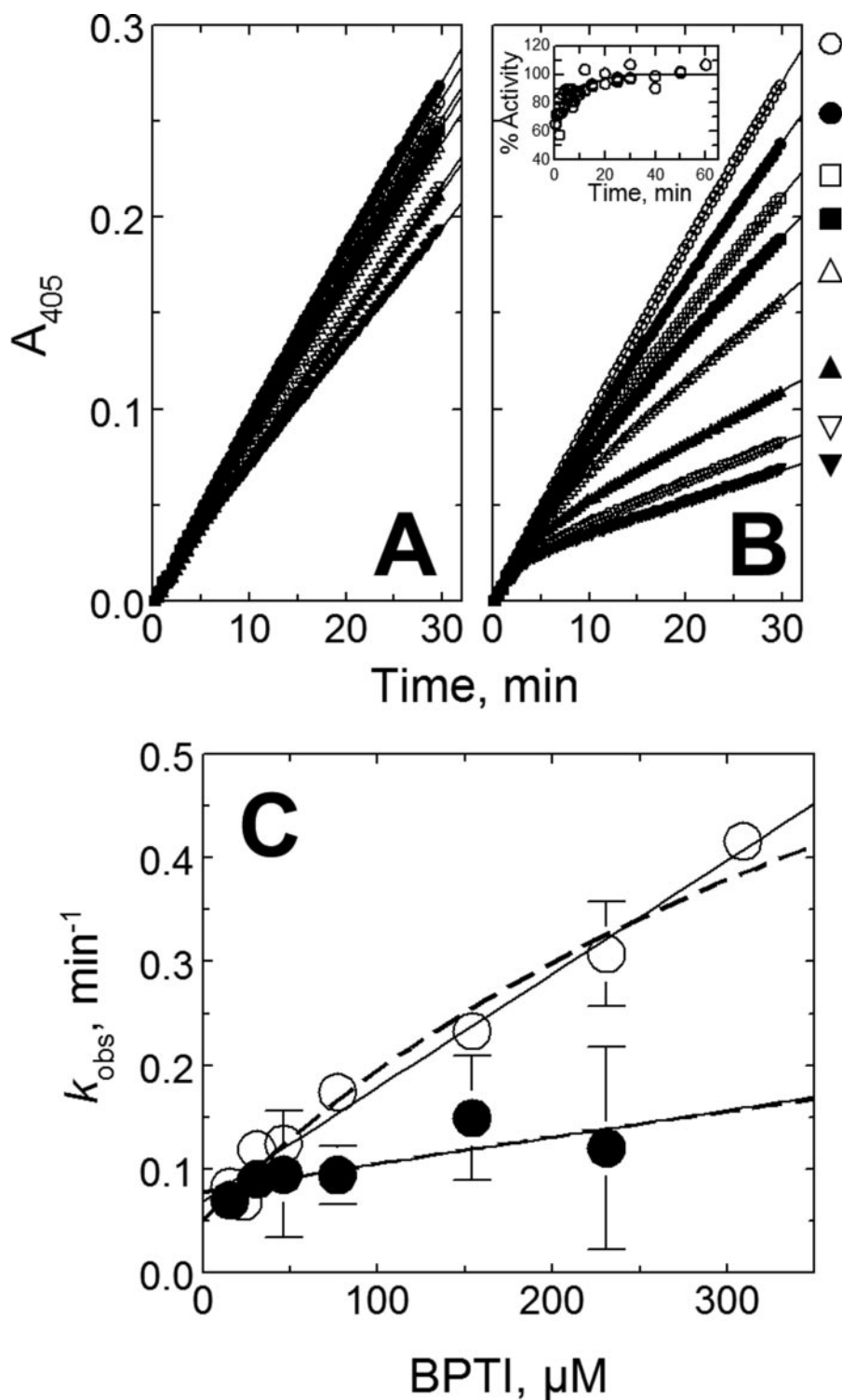| Enzyme | $K_m$ | $k_{cat}$ | $k_{cat}/K_m$ |
|---|---|---|---|
| | M | s$^{-1}$ | M$^{-1}$ s$^{-1}$ |
| WT fIXa | $3.78 (\pm 0.08) \times 10^{-3}$ | $16.5 (\pm 0.69)$ | $4.37 (\pm 0.08) \times 10^3$ |
| fIXaK98A | $1.58 (\pm 0.02) \times 10^{-3}$ | $6.23 (\pm 0.43)$ | $3.98 (\pm 0.27) \times 10^3$ |

FIGURE 6. **Slow-binding inhibition of WT fIXa by BPTI.** *A*, progress curves of WT fIXa inhibition by BPTI in the absence of enoxaparin. *B*, progress curves of WT fIXa inhibition by BPTI in the presence of 10 μM enoxaparin. BPTI concentrations used were: 0 (○), 15.4 (●), 30.8 (□), 46.2 (■), 77 (△), 154 (▲), 231 (▽), and 308 μM (▼). *Inset*, recovery of enzymatic activity of WT fIXa after inhibition with BPTI and enoxaparin. The inhibited fIXa-BPTI complex was diluted 1,000-fold and timed aliquots were removed into CBS 31.39 substrate to measure recovery of enzymatic activity over time. The activities were compared with a parallel reaction done in the absence of inhibitor to normalize values to 100%. The data were fitted with a single-exponential equation to determine a value for *k* (roughly equivalent to $k_{10}$, see text). *C*, secondary plots of $k_{obs}$ from *panels A* and *B versus* BPTI concentration for WT fIXa in the absence (●) and presence (○) of enoxaparin. Data were fitted with Equation 5 (*solid lines*). Kinetic constants obtained are given in Table 2. Refitting of the data using Equation 4 as described under "Discussion" is also shown (*dashed lines*).

concentrations (*cf.* Fig. 6, *A* and *B*) are diagnostic for Scheme Ib. The data of Fig. 6*C* were thus fitted with Equation 5 to obtain estimates for the apparent second-order rate constant; $k_9 = 5.4$ M$^{-1}$ s$^{-1}$ without enoxaparin and 23 M$^{-1}$ s$^{-1}$ with enoxaparin. The value obtained above for $k_6$ ($k_{10}$ in Scheme Ib) is consistent with the values obtained for $k_{10}$ using Equation 5; $k_{10} = 1.3 \times 10^{-3}$ s$^{-1}$ without enoxaparin and $1.2 \times 10^{-3}$ s$^{-1}$ with enoxaparin.

A similar slow-binding kinetic analysis was performed with WT fIXa and PN2-KPI. In contrast to what was observed with BPTI, secondary plots of $k_{obs}$ *versus* PN2-KPI were hyperbolic (not shown) and well described by Scheme Ia, yielding the values of $K_i$, $k_5$, and $k_6$ given in Table 2. The role of Lys[98] and the 99-loop of fIXa in inhibition of fIXa by both BPTI and PN2-KPI were next examined using fIXaK98A. This mutant fIXa showed increased reactivity toward all of the inhibitors examined (Table 3). More importantly, the enhancing effect of enoxaparin was substantially reduced when compared with WT fIXa. Detailed analysis of the slow-binding kinetics of inhibition of fIXaK98A by BPTI revealed that the major difference compared with WT fIXa was the enhanced formation of the initial enzyme-inhibitor complex, as seen visually by the variation in initial rate ($v_o$) of progress curves (Fig. 7, *A* and *B*) and the hyperbolic nature of secondary plots (Fig. 7*C*). Although enoxaparin significantly enhanced the reactivity of both WT fIXa and fIXaK98A toward BPTI (Table 2), the effect on the mutant was much reduced and was completely abrogated for its inhibition by PN2-KPI.

## DISCUSSION

Previous studies by us have demonstrated that heparin binding to fIXa enhances fIXa reactivity with BPTI (15). Whereas in that study unfractionated heparin was found to have a slightly greater effect, enoxaparin retained most of the ability to enhance fIXa reactivity.

**TABLE 2**

**Kinetic constants for inhibition of fIXa and fIXaK98A by BPTI and PN2-KPI**

Unless indicated otherwise, values of kinetic constants were obtained using Equations 3 and 4 (see text).

| Enzyme | Inhibitor | Enoxaparin | $K_i$ | $k_5$ | $k_9$ | $k_6$ or $k_{10}$[a] | $K_i^*{}_{calc}$[b] |
|---|---|---|---|---|---|---|---|
| | | | $M$ | $s^{-1}$ | $M^{-1} s^{-1}$ | $s^{-1}$ | $M$ |
| WT fIXa | BPTI | − | $2.1 \times 10^{-3}$ [c] | | $5.4$ | $2.67 (\pm 1.50) \times 10^{-3}$ | |
| | | + | $4.1 \times 10^{-4}$ [c] | | $23$ | $1.17 (\pm 0.17) \times 10^{-3}$ | |
| | PN2-KPI | − | $2.0 \times 10^{-5}$ | $1.3 \times 10^{-2}$ | | $3.67 (\pm 2.66) \times 10^{-3}$ | $4.4 \times 10^{-6}$ |
| | | + | $3.3 \times 10^{-5}$ | $1.3 \times 10^{-2}$ | | $3.50 (\pm 0.67) \times 10^{-3}$ | $7.0 \times 10^{-6}$ |
| fIXaK98A | BPTI | − | $1.3 \times 10^{-4}$ | $1.5 \times 10^{-2}$ | | $2.33 (\pm 0.67) \times 10^{-3}$ | $1.7 \times 10^{-5}$ |
| | | + | $8.8 \times 10^{-5}$ | $1.6 \times 10^{-2}$ | | $1.65 (\pm 0.33) \times 10^{-3}$ | $8.2 \times 10^{-6}$ |
| | PN2-KPI | − | $6.8 \times 10^{-6}$ | $1.4 \times 10^{-2}$ | | $2.33 (\pm 1.00) \times 10^{-3}$ | $9.7 \times 10^{-7}$ |
| | | + | $8.0 \times 10^{-6}$ | $1.4 \times 10^{-2}$ | | $2.00 (\pm 0.83) \times 10^{-3}$ | $1.0 \times 10^{-6}$ |

[a] Values are $k_{10}$ for WT fIXa with BPTI (Scheme Ib) and $k_6$ for others (Scheme Ia) $\pm$ S.D. ($n \geq 7$).
[b] Calculated from $k_5$, $k_6$, and $K_i$ using the relationship $K_i^* = k_6 \cdot K_i / (k_5 + k_6)$ (33, 34).
[c] Determined from refits of the data in Fig. 6C with Equation 4 using $k_5$ obtained for fIXaK98A and BPTI (see "Discussion").

**TABLE 3**

**Equilibrium inhibition constants for Kunitz-type inhibitors and WT fIXa *versus* fIXaK98A**

| Enzyme | Enoxaparin | $K_{i,eq}$ | | | |
|---|---|---|---|---|---|
| | | BPTI | TFPI-K1 | TFPI-K2 | PN2-KPI |
| | | | $M$ | | |
| WT fIXa | − | $6.46 (\pm 0.83) \times 10^{-4}$ | $>1.0 \times 10^{-3}$ | $4.14 (\pm 0.51) \times 10^{-4}$ | $9.52 (\pm 1.0) \times 10^{-6}$ |
| | + | $5.91 (\pm 0.32) \times 10^{-5}$ | $>1.0 \times 10^{-3}$ | $2.57 (\pm 0.71) \times 10^{-4}$ | $6.84 (\pm 0.76) \times 10^{-6}$ |
| fIXaK98A | − | $2.48 (\pm 0.54) \times 10^{-5}$ | $1.31 (\pm 0.23) \times 10^{-4}$ | $4.36 (\pm 0.51) \times 10^{-5}$ | $1.31 (\pm 0.17) \times 10^{-6}$ |
| | + | $1.32 (\pm 0.24) \times 10^{-5}$ | $1.11 (\pm 0.42) \times 10^{-4}$ | $2.83 (\pm 0.11) \times 10^{-5}$ | $1.19 (\pm 0.19) \times 10^{-6}$ |

The conclusion that heparin can modulate the active site of fIXa is supported in the present study by several observations, not the least of which is the ability of short chain oligosaccharides to retain the ability to enhance fIXa reactivity with BPTI. Whereas the shortest oligosaccharide examined (H6) requires higher concentrations than do H10–H18, the higher $IC_{50}$ for H6 is consistent with the reduced binding energy one may expect for a small oligosaccharide whose projected length would contact only two thirds of the heparin binding exosite: based on available crystal structures (Protein Data Bank codes 1E0O and 1BFC) the length of a decasaccharide is expected to be ~38 Å and that of a hexasaccharide is expected to be ~23 Å at full extension. This is compared with the measured length of the identified heparin binding site on fIXa (~35 Å) based on mutational studies (14).

With respect to the inhibition of fIXa by BPTI, two main conclusions may be drawn from these studies: 1) fIXa residue Lys[98] is in part responsible for protecting fIXa from inhibition by BPTI, likely via steric hindrance. Removal of this steric obstruction by mutation of Lys[98] results in greater inhibition of fIXa by BPTI (26-fold enhancement). 2) Heparin binding to fIXa in part counteracts the steric protection provided by Lys[98]. Mutation of Lys[98] results in a reduction in the ability of heparin to further enhance reactivity of fIXa with BPTI (roughly 2-fold effect for fIXaK98A compared with >10-fold effect with WT fIXa). The lack of complete abrogation of the effect of heparin suggests that other as yet undefined factors also play a role in BPTI inhibition of fIXa and its response to heparin. This is likely due to the movement of more than simply Lys[98] and may or may not involve other residues in the 99-loop or even the entire loop.

It is important to note that the reduction in the effect of heparin with the fIXaK98A mutant is not merely due to reduced heparin binding because fIXaK98A retained the ability to bind to heparin-Sepharose and eluted at the same salt con-

centration as WT fIXa during purification procedures. In support of this, preliminary experiments performed by titrating fIXaK98A with enoxaparin in the presence of 100 $\mu$M BPTI yielded results consistent with the high nanomolar affinity for enoxaparin previously observed with fIXa$\beta$ ($K_d$ = 128 nM (15)). No further increase in inhibition of fIXaK98A by BPTI was observed when the enoxaparin level was increased from 1 to 10 $\mu$M (not shown). Because all experiments were conducted using 10 $\mu$M enoxaparin, it seems reasonable to assume that fIXaK98A was saturated in these experiments.

Whereas the data for fIXa with BPTI in Fig. 6C are consistent with Scheme Ib, this scheme is essentially a simplified version of Scheme Ia with a very large value for $K_i$ (33, 34). Examination of the Scheme Ia kinetic constants in Table 3 for fIXa with PN2-KPI as well as those for fIXaK98A with both inhibitors shows fairly consistent values for $k_5$ and $k_6$. This suggests that once formed, isomerization of the $EI$ complex to $EI^*$ is essentially the same for any of the enzyme-inhibitor pairs examined. Based on this it seems reasonable to tentatively extend the value of $k_5$ to the WT fIXa-BPTI pair and re-examine the data of Fig. 6C with respect to Scheme Ia. This results in fits to Equation 4 shown in Fig. 6C as *dashed lines* and yields initial $K_i$ values of $2.1 \times 10^{-3}$ M and $4.1 \times 10^{-4}$ M in the absence and presence of enoxaparin, respectively. This 5-fold difference in $K_i$ along with ~2-fold difference in $k_6$ ($k_{10}$) for this enzyme-inhibitor pair (Table 2) would seem to account for the ~10-fold effect of enoxaparin observed in $K_{i,eq}$ (Table 3). Unfortunately, the rather large errors in the values of $k_6$ ($k_{10}$) preclude definitive conclusions concerning potential effects of enoxaparin on this rate constant.

Regardless, these results are consistent with a very weak initial interaction of fIXa with BPTI. Enoxaparin binding to the heparin binding exosite in fIXa at least in part acts to allosterically modulate the 99-loop of fIXa in a manner that facilitates this initial interaction. The results with BPTI are in contrast to
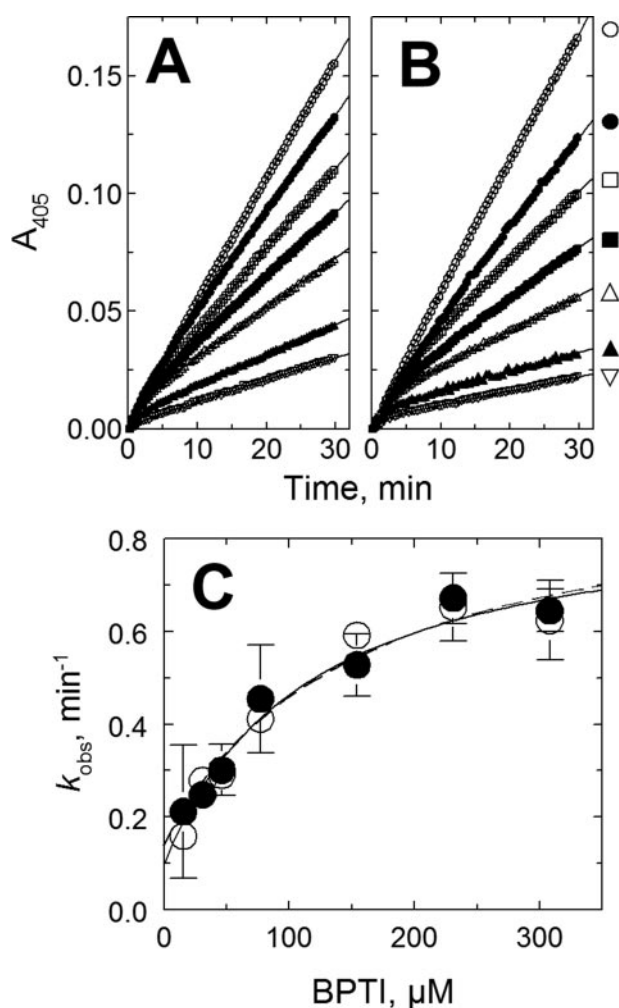
FIGURE 7. **Slow-binding inhibition of fIXaK98A by BPTI.** *A*, progress curves of fIXaK98A inhibition by BPTI in the absence of enoxaparin. *B*, progress curves of fIXaK98A inhibition by BPTI in the presence of 10 $\mu$M enoxaparin. BPTI concentrations used were: 0 (○), 15.4 (●), 30.8 (□), 46.2 (■), 77 (△), 154 (▲), and 231 $\mu$M (▽). *C*, secondary plots of $k_{obs}$ from *panels A* and *B versus* BPTI concentration for fIXaK98A in the absence (●) and presence (○) of enoxaparin. Data were fitted with Equation 4 (*lines*). Kinetic constants obtained are given in Table 2.

the interaction of fIXa with TFPI-K1, TFPI-K2, or PN2-KPI. The former shows no effect of heparin binding, whereas the latter two show only small (but reproducible) responses to heparin binding. These results would suggest that these three Kunitz inhibitor domains are not as greatly hindered as BPTI by the 99-loop of fIXa. Indeed, mutation of Lys[98] enhanced the inhibition by TFPI-K1 roughly 8-fold, TFPI-K2 roughly 9-fold, and by PN2-KPI only 6–7-fold. Interestingly, however, the effect of enoxaparin on fIXaK98A reactivity toward both TFPI-K1 and TFPI-K2 was unchanged, whereas that for PN2-KPI was completely abrogated. Thus, there is some disparity in the role of Lys[98] and additional effects of heparin binding are likely.

Previous studies have demonstrated the ability of full-length TFPI to inhibit fIXa with an affinity of roughly 300 nM (40). It is thus interesting that neither the isolated TFPI-K1 nor isolated TFPI-K2 domains retain very high reactivity with fIXa. Preliminary studies indicated that our preparations of isolated inhibitor domains were of good quality and activity. This would seem to indicate that the folding and activity of these inhibitor

domains are correct. Taken as a whole, the results here would seem to imply that either the connecting regions of TFPI are important for its activity toward fIXa or other structural/topological elements are involved. Nonetheless, it is likely that the TFPI-K2 domain is the inhibitor domain of TFPI most likely responsible for interaction with fIXa. Although the isolated third Kunitz repeat of TFPI was not examined in this study, this domain is likely not an active inhibitor domain *per se* (41).

The ability of heparin to allosterically modulate the active site of fIXa demonstrates the ability of fIXa to respond to binding at this exosite. This observation is made more interesting by the observation by Sheehan *et al.* (42, 43) that the heparin binding exosite in part represents a fVIIIa interactive site on fIXa. Thus, whereas heparin binding in itself may inhibit fIXa coagulant activity via steric hindrance of fVIIIa binding, fVIIIa binding to this exosite may inversely act to allosterically modulate fIXa in an as yet undefined manner. Although previous studies found no effect of fVIIIa on fIXa inhibition by the isolated PN2-KPI domain (44), this is consistent with our observations here using enoxaparin in place of fVIIIa and does not preclude potential effects of fVIIIa toward other inhibitors. It thus remains possible that occupation of this exosite by fVIIIa, like heparin, results in inhibitor-specific modulatory effects. Alternatively, the modulating effect of heparin on the 99-loop may be simply due to heparin-specific electrostatic forces that are introduced by heparin binding in close proximity to Lys[98] (*cf.* Fig. 4). These forces may or may not be mimicked by fVIIIa binding. Further clarification of these issues must await future studies.

The allosteric modulation of fIXa by enoxaparin is somewhat reminiscent of the effect of thrombomodulin on the interaction of thrombin with BPTI, where binding of thrombomodulin alters the conformation of one of the specificity loops (60-loop) at the mouth of the active site of thrombin, resulting in enhanced reactivity with BPTI (45). Interestingly, in that study the chondroitin sulfate moiety of thrombomodulin (which binds to the heparin binding site on thrombin; anion binding exosite 2) further enhanced the inhibition of an E192Q mutant of thrombin but not wild-type thrombin. Comparison of the sequence of fIXa with thrombin reveals that fIXa contains a Gln at position 192, similar to the thrombin E192Q mutant and fXa. In addition, previous studies have revealed that mutation of the homologous residue in fVIIa (Lys[192]) to Gln enhances its reactivity with BPTI (29), and that mutation of Gln[192] in fIXa altered its reactivity toward TFPI (40). Neither of these studies examined the potential effect of heparin on reactivity with these Kunitz inhibitors. These studies are intriguing and seem to implicate residue 192 in potential heparin responsiveness along with the 99-loop. The investigation of potential interplay between residue 192 and the 99-loop of fIXa in its response to heparin binding is beyond the scope of the present study, however, and must await future studies.
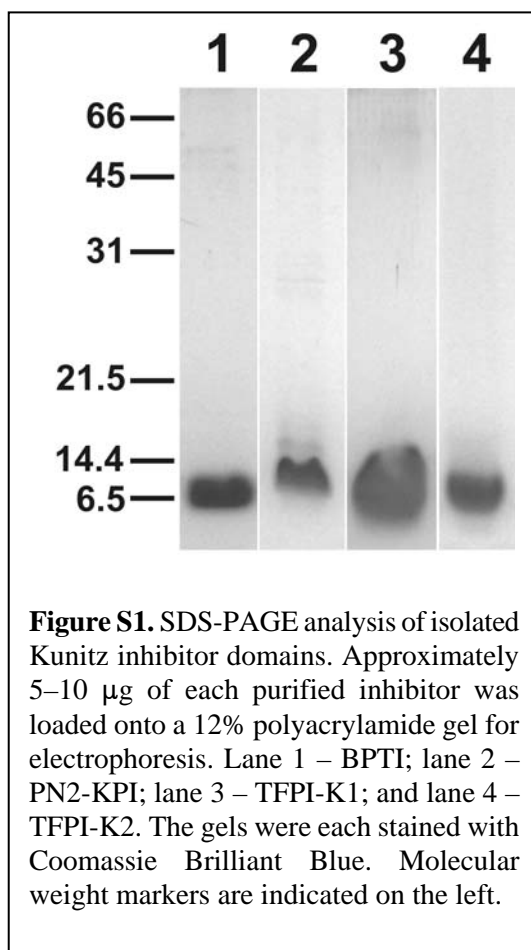
## REFERENCES

1. Neuenschwander, P. (2006) in *Encyclopedia of Respiratory Medicine* (Laurant, G., and Shapiro, S., eds) pp. 509–514, Elsevier Ltd., Oxford, UK
2. Jesty, J., and Nemerson, Y. (1995) in *Williams Hematology* (Beutler, E., Lichtman, M. A., Collar, B. S., and Kipps, T. J., eds) 5th Ed., pp. 1227–1238, McGraw-Hill, Inc., New York
3. van Dieijen, G., Tans, G., Rosing, J., and Hemker, H. C. (1981) *J. Biol. Chem.* **256,** 3433–3442
4. van Dieijen, G., van Rijn, J. L., Govers-Riemslag, J. W., Hemker, H. C., and Rosing, J. (1985) *Thromb. Haemostasis* **53,** 396–400
5. Mertens, K., and Bertina, R. M. (1984) *Biochem. J.* **223,** 607–615
6. Mertens, K., van Wijngaarden, A., and Bertina, R. M. (1985) *Thromb. Haemostasis* **54,** 654–660
7. Rosenberg, J. S., McKenna, P. W., and Rosenberg, R. D. (1975) *J. Biol. Chem.* **250,** 8883–8888
8. Kurachi, K., Fujikawa, K., Schmer, G., and Davie, E. W. (1976) *Biochemistry* **15,** 373–377
9. DiScipio, R. G., Kurachi, K., and Davie, E. W. (1978) *J. Clin. Investig.* **60,** 1528–1538
10. Villaneuva, G. B., and Danishefsky, I. (1977) *Biochem. Biophys. Res. Commun.* **74,** 803–809
11. Villaneuva, G. B. (1984) *J. Biol. Chem.* **259,** 2531
12. Olson, S. T., and Björk, I. (1992) *Adv. Exp. Med. Biol.* **313,** 155–165
13. Olson, S. T., Björk, I., Sheffer, R., Craig, P. A., Shore, J. D., and Choay, J. (1992) *J. Biol. Chem.* **267,** 12528–12538
14. Yang, L. K., Manithody, C., and Rezaie, A. R. (2002) *J. Biol. Chem.* **277,** 50756–50760
15. Neuenschwander, P. F. (2004) *Biochemistry* **43,** 2978–2986
16. Rezaie, A. R., Fiore, M. M., Neuenschwander, P. F., Esmon, C. T., and Morrissey, J. H. (1992) *Protein Expression Purif.* **3,** 453–460
17. Neuenschwander, P. F., and Morrissey, J. H. (1994) *J. Biol. Chem.* **269,** 8007–8013
18. Olson, S. T., Björk, I., and Shore, J. D. (1993) in *Methods in Enzymology* (Lorand, L., and Mann, K. G., eds) pp. 525–559, Academic Press, New York
19. Lindahl, U., Thunberg, L., Bäckström, G., Riesenfeld, J., Nordling, K., and Björk, I. (1984) *J. Biol. Chem.* **259,** 12368–12376
20. Olson, S. T. (1988) *J. Biol. Chem.* **263,** 1698–1708
21. Anderer, F. A. (1965) *Z. Naturforsch. B* **20,** 462–472
22. Anderer, F. A., and Hoernle, S. (1965) *Z. Naturforsch. B* **20,** 457–462
23. Wagner, S. L., Siegel, R. S., Vedvick, T. S., Raschke, W. C., and Van Nostrand, W. E. (1992) *Biochem. Biophys. Res. Commun.* **186,** 1138–1145
24. Wun, T. C., Kretzmer, K. K., Girard, T. J., Miletich, J. P., and Broze, G. J., Jr. (1988) *J. Biol. Chem.* **263,** 6001–6004
25. Steinle, A., Li, P., Morris, D. L., Groh, V., Lanier, L. L., Strong, R. K., and Spies, T. (2001) *Immunogenetics* **53,** 279–287
26. De Bernardez Clark, E., Hevehan, D., Szela, S., and Maachupalli-Reddy, J. (1998) *Biotechnol. Prog.* **14,** 47–54
27. Kurachi, K., and Davie, E. W. (1982) *Proc. Natl. Acad. Sci. U. S. A.* **79,** 6461–6464
28. Horton, R. M., Cai, Z., Ho, S. N., and Please, L. R. (1990) *BioTechniques* **8,** 528–535
29. Neuenschwander, P. F., and Morrissey, J. H. (1995) *Biochemistry* **34,** 8701–8707
30. Chase, T., Jr., and Shaw, E. (1967) *Biochem. Biophys. Res. Commun.* **29,** 508–514
31. Mann, K. G., Williams, E. B., Krishnaswamy, S., Church, W., Giles, A., and Tracy, R. P. (1990) *Blood* **76,** 755–766
32. Neuenschwander, P. F., McCollough, J., McCallum, C. D., and Johnson, A. E. (1997) *Thromb. Haemostasis* **78,** (suppl.) 428
33. Morrison, J. F., and Walsh, C. T. (1988) *Adv. Enzymol.* **61,** 201–301
34. Copeland, R. A. (1996) *Enzymes: A Practical Introduction to Structure, Mechanism, and Data Analysis*, pp. 225–261, VCH Publishers, Inc., New York
35. Van Nostrand, W. E., Wagner, S. L., Farrow, J. S., and Cunningham, D. S. (1990) *J. Biol. Chem.* **265,** 9591–9594
36. Petersen, L. C., Bjorn, S. E., Olsen, O. H., Nordfang, O., Norris, F., and Norris, K. (1996) *Eur. J. Biochem.* **235,** 310–316
37. Wlodawer, A., Walter, J., Huber, R., and Sjolin, L. (1984) *J. Mol. Biol.* **180,** 301–329
38. Hopfner, K. P., Lang, A., Karcher, A., Sichler, K., Kopetzki, E., Brandstetter, H., Huber, R., Bode, W., and Engh, R. A. (1999) *Struct. Fold Des.* **7,** 989–996
39. Zhang, E., St. Charles, R., and Tulinsky, A. (1999) *J. Mol. Biol.* **285,** 2089–2104
40. Hsu, Y. C., Hamaguchi, N., Chang, Y. J., and Lin, S. W. (2001) *Biochemistry* **40,** 11261–11269
41. Piro, O., and Broze, G. J., Jr. (2004) *Circulation* **110,** 3567–3572
42. Yuan, Q. P., Walke, E. N., and Sheehan, J. P. (2005) *Biochemistry* **44,** 3615–3625
43. Sheehan, J. P., Kobbervig, C. E., and Kirkpatrick, H. M. (2003) *Biochemistry* **42,** 11316–11325
44. Schmaier, A. H., Dahl, L. D., Hasan, A. A. K., Cines, D. B., Bauer, K. A., and Van Nostrand, W. E. (1995) *Biochemistry* **34,** 1171–1178
45. Rezaie, A. R., He, X., and Esmon, C. T. (1998) *Biochemistry* **37,** 693–699

HEPARIN MODULATES THE 99-LOOP OF FACTOR IXA: EFFECTS ON REACTIVITY WITH ISOLATED
KUNITZ-TYPE INHIBITOR DOMAINS
Neuenschwander, P.F., Williamson, S.R., Nalian, A. and Baker-Deadmond, K.J.

**Table S1.** Amino Acid Sequence Alignment of Kunitz-type inhibitor domains[*]

|  | 1 | 10 | 20 | 30 | 40 | 50 |
|---|---|---|---|---|---|---|
| **BPTI** | RPDFCLEPPYTGPC**K**ARIIRYFYNAKAGLCQTFVYGGCRAKRNNFKSAEDCMRTCGGA |
| **PN2-KPI** | EVVREVCSEQAETGPC**R**AMISRWYFDVTEGKCAPFFYGGCGGNRNNFDTEEYCMAVCGSA |
| **TFPI-K1** | MHSFCAFKADDGPC**K**AIMKRFFFNIFTRQCEEFIYGGCEGNQNRFESLEECKKMCTRD |
| **TFPI-K2** | KPDFCFLEEDPGIC**R**GYITRYFYNNQTKQCERFKYGGCLGNMNNFETLEECKNICEDG |
| **TFPI-K3** | GPSWCLTPADRGLC**R**ANENRFYYNSVIGKCRPFKYSGCGGNENNFTSKQECLRACKK |

[*]Conserved amino acids with BPTI are shaded. Reactive site loops (thin boxes) and stabilizing loops (thick boxes) are held in close proximity by a disulfide bond between $Cys_{14}$ and $Cys_{38}$ (indicated). The P1 reactive site residues are in bold.



**Figure S1.** SDS-PAGE analysis of isolated Kunitz inhibitor domains. Approximately 5–10 μg of each purified inhibitor was loaded onto a 12% polyacrylamide gel for electrophoresis. Lane 1 – BPTI; lane 2 – PN2-KPI; lane 3 – TFPI-K1; and lane 4 – TFPI-K2. The gels were each stained with Coomassie Brilliant Blue. Molecular weight markers are indicated on the left.

SUPPLEMENTAL DATA
HEPARIN MODULATES THE 99-LOOP OF FACTOR IXA: EFFECTS ON REACTIVITY WITH ISOLATED
KUNITZ-TYPE INHIBITOR DOMAINS
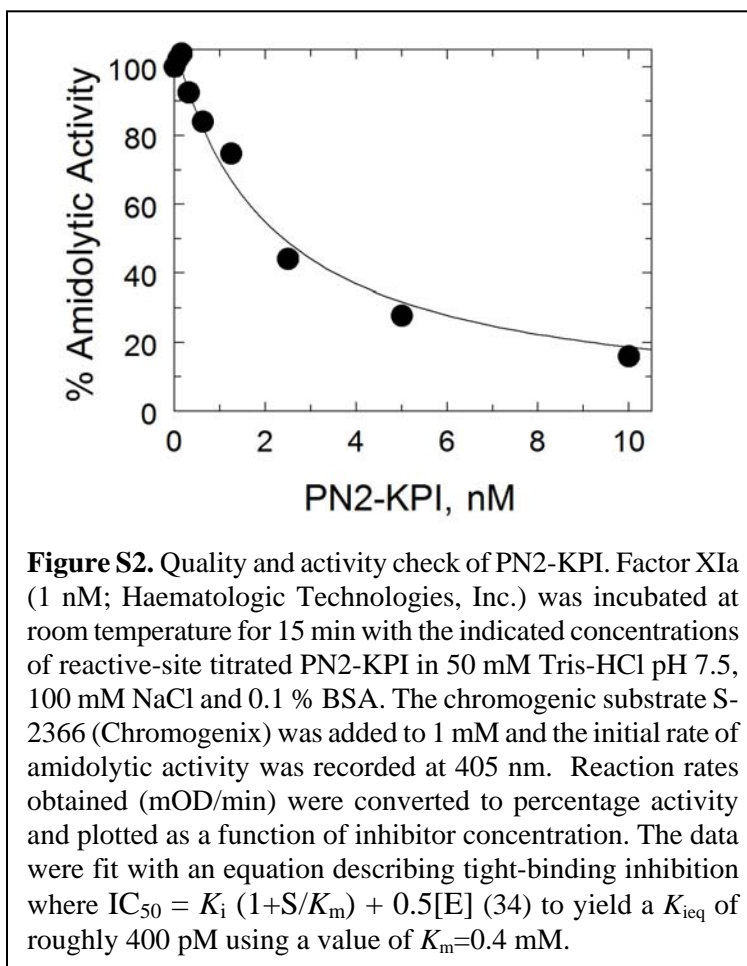Neuenschwander, P.F., Williamson, S.R., Nalian, A. and Baker-Deadmond, K.J.



**Figure S2.** Quality and activity check of PN2-KPI. Factor XIa (1 nM; Haematologic Technologies, Inc.) was incubated at room temperature for 15 min with the indicated concentrations of reactive-site titrated PN2-KPI in 50 mM Tris-HCl pH 7.5, 100 mM NaCl and 0.1 % BSA. The chromogenic substrate S-2366 (Chromogenix) was added to 1 mM and the initial rate of amidolytic activity was recorded at 405 nm.  Reaction rates obtained (mOD/min) were converted to percentage activity and plotted as a function of inhibitor concentration. The data were fit with an equation describing tight-binding inhibition where $IC_{50} = K_i (1+S/K_m) + 0.5[E]$ (34) to yield a $K_{ieq}$ of roughly 400 pM using a value of $K_m=0.4$ mM.

HEPARIN MODULATES THE 99-LOOP OF FACTOR IXA: EFFECTS ON REACTIVITY WITH ISOLATED
KUNITZ-TYPE INHIBITOR DOMAINS
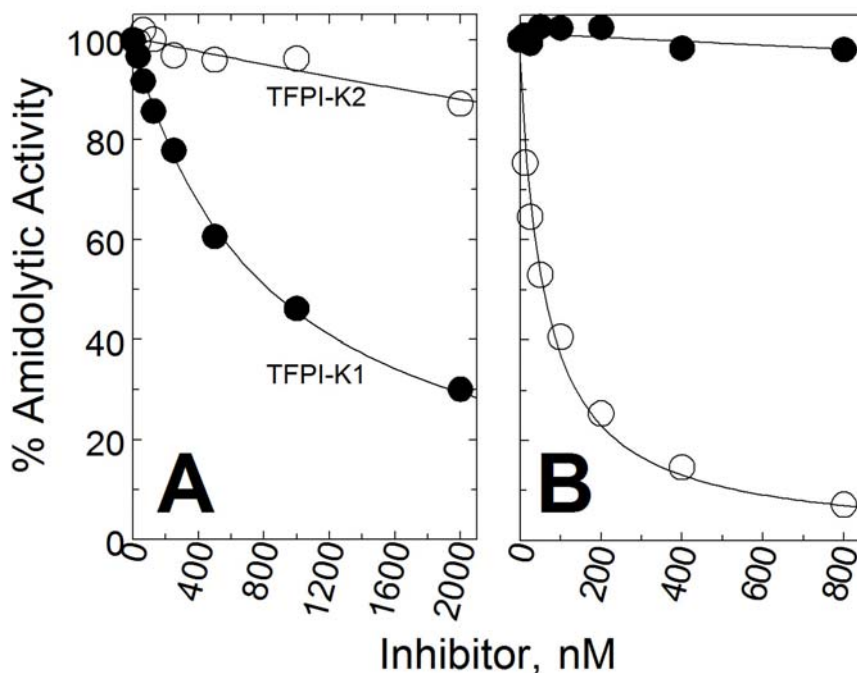Neuenschwander, P.F., Williamson, S.R., Nalian, A. and Baker-Deadmond, K.J.



**Figure S3.** Quality and activity check of TFPI-K1 and TFPI-K2. *A*. Inhibition of the complex of factor VIIa and soluble tissue factor. The indicated concentrations of TFPI-K1 (●) or TFPI-K2 (○) were incubated with 5 nM factor VIIa (Haematologic Technologies, Inc.) , 100 nM recombinant soluble tissue factor (16) and 5 mM $Ca^{2+}$ in 20 mM Hepes-NaOH pH 7.4, 100 mM NaCl and 0.1% BSA for 15 minutes at room temperature as previously described (24). The chromogenic substrate Chromozym-tPA (Roche Diagnostics) was then added to 1 mM and the initial rate of amidolytic activity was monitored at 405 nm. Reaction rates obtained (mOD/min) were converted to percentage activity and plotted as a function of inhibitor concentration. Fits of the data with Equation 1 yielded $K_{ieq}$ values of 400 nM for TFPI-K1 and ~7 µM for TFPI-K2. *B*. Inhibition of factor Xa. The indicated concentrations of TFPI-K1 (●) or TFPI-K2 (○) were incubated with 5 nM factor Xa and 5 mM $Ca^{2+}$ in 20 mM Hepes-NaOH pH 7.4, 100 mM NaCl and 0.1% BSA for 15 minutes at room temperature. The chromogenic substrate S-2222 (Chromogenix) was then added to 0.5 mM and the initial rate of amidolytic activity was monitored at 405 nm. Reaction rates (mOD/min) were converted to percentage activity and plotted as a function of inhibitor concentration. Fits of the data with Equation 1 yielded $K_{ieq}$ values of >1.5 µM for TFPI-K1 and 24 nM for TFPI-K2.